ELSEVIER

Biochemical Pharmacology 63 (2002) 1061–1068

Biochemical Pharmacology

A glutamate-gated chloride channel subunit from *Haemonchus contortus*: Expression in a mammalian cell line, ligand binding, and modulation of anthelmintic binding by glutamate

Sean G. Forrester, Roger K. Prichard, Robin N. Beech*

Institute of Parasitology, McGill University, 21,111 Lakeshore Road, Ste-Anne-de-Bellevue, Que., Canada H9X 3V9

Received 22 March 2001; accepted 16 August 2001

Abstract

Glutamate-gated chloride channels (GluCls) are inhibitory ion channels that are sensitive to the antiparasitic drugs ivermectin (IVM) and moxidectin (MOX). We have transiently transfected COS-7 cells with a subunit of a GluCl (HcGluCla) from the parasitic nematode *Haemonchus contortus*. This subunit bound [^{3}H]-IVM and [^{3}H]-MOX with K_d values of 0.11 ± 0.021 and 0.18 ± 0.02 nM, respectively. Displacement analysis revealed that IVM and MOX bind to the same site on HcGluCla and that this site is likely distinct from the glutamate binding site. Glutamate was found to be an allosteric modulator of [^{3}H]-MOX and [^{3}H]-IVM binding and increased the affinity of [^{3}H]-MOX for HcGluCla by more than 50% and that of [^{3}H]-IVM by more than 7-fold. These results point to both similarities and differences in the interactions of IVM and MOX with the GluCl. Aspartate, which is structurally similar to glutamate, had little or no effect on [^{3}H]-IVM and [^{3}H]-MOX binding, suggesting that this ligand does not induce the conformational change necessary to potentiate macrocyclic lactone binding. These results also indicate that it may be possible to enhance the efficacy of macrocyclic lactone anthelmintics by administering these compounds with ligands acting allosterically to enhance their binding.

Keywords: Glutamate; Ion channel; Neurotransmitter receptor; Moxidectin; Ivermectin; Anthelmintic

1. Introduction

The neurotransmitter glutamate and the antiparasitic agent IVM are agonists for an inhibitory ligand-gated ion channel, the GluCl [1–4]. These channels, found only in invertebrates, have been characterized from *Caenorhabditis elegans* [5–12], *Drosophila melanogaster* [13], and *Ascaris suum* [14], and their genes have been cloned from the parasitic nematode *Haemonchus contortus* [15–18]. GluCla subunits, expressed in *Xenopus* oocytes, form homomeric channels that are generally gated by L-glutamate, ibotenate, and IVM [7,9,10,13], and, like the GABA- and glycine-gated chloride channels [19,20], are blocked by picrotoxin [21]. GluCls do not respond to aspartate, quisqualate, or *N*-methyl-D-aspartic acid [7].

There have been numerous studies on the effects of avermectins, such as IVM, on the GluCla. However, little is known about the interaction of this channel with the structurally similar milbemycins, such as MOX. Martin [14] showed evidence for a milbemycin D-sensitive GluCl in the pharynx of *A. suum*, suggesting that this group of compounds shares a similar mode of action with the avermectins. Both anthelmintic structures share a 16-membered macrocyclic unit, but differ in the fact that the avermectins possess a disaccharide substituent at C-13 that is not present in the milbemycins, while MOX is substituted at C-23 and C-25 compared with IVM [22]. Although the milbemycins and the avermectins do share similarities in their structures, some reports suggest that MOX is effective in treating nematode infections when IVM fails [23,24], suggesting that the two compounds show some differences in their action. Others, however, have reported cross-resistance between IVM and MOX [25]. It is now generally accepted that IVM acts on GluCl channels. However, it is not known whether MOX exhibits interactions with the GluCl identical to those of IVM.

* Corresponding author. Tel.: +1-514-398-7535; fax: +1-514-398-7857.
E-mail address: robin.beech@mcgill.ca (R.N. Beech).

Abbreviations: GluCls, glutamate-gated chloride channels; HcGluCla, *Haemonchus contortus* glutamate-gated chloride channel subunit; IVM, ivermectin; MOX, moxidectin; COS-7, African green monkey kidney cells; GABA, γ-aminobutyric acid; TBS, Tris-buffered saline.

0006-2952/02/$ – see front matter
PII: S0006-2952(02)00852-3

Furthermore, on a broad scale, it is still unconfirmed whether these anthelmintics share identical modes of action and mechanisms of resistance.

GluCla homomeric or αβ heteromeric channels expressed in *Xenopus* oocytes are directly activated by glutamate and IVM [7,10]. However, IVM binds at a much higher affinity than glutamate, and it has been shown that the two ligands share an allosteric interaction [7]. For instance, when *C. elegans* GluCls are treated initially with IVM, the glutamate response is increased, suggesting that IVM potentiates glutamate activity [6,7]. On the other hand, Cully *et al.* [13] observed an inhibitory effect of IVM on glutamate activity on a *D. melanogaster* GluCla channel, and Paiement *et al.* [26] found that IVM inhibits glutamate binding to *H. contortus* membrane preparations. These inhibitory effects of IVM may be due to interactions with the glutamate binding site or more likely through an allosteric interaction from a distinct site. Moreover, what effect glutamate has on IVM/MOX activity is still unknown. Further studies on the interaction between glutamate and the macrocyclic lactones on the GluCl will provide more information on the nature of the macrocyclic lactone binding site, the activity of these anthelmintics, and the potential differences in activity between the avermectins and milbemycins.

In the present study, we have utilized the mammalian COS-7 expression system to examine the ligand binding properties of a GluCl subunit (HcGluCla) from the parasitic nematode *H. contortus*. We report evidence that HcGluCla is a subunit that exhibits separate binding sites for glutamate and IVM/MOX. We also report new findings that glutamate potentiates IVM/MOX binding to this GluCl subunit. This is the first demonstration of enhanced anthelmintic binding by ligands acting allosterically at the same receptor.

2. Materials and methods

2.1. Chemicals

[^{3}H]-IVM (18.6 Ci/mmol) was a gift from Merck Research Laboratories, and [^{3}H]-MOX (48 Ci/mmol) was a gift from Fort Dodge Animal Health. L-Glutamate was purchased from Research Biochemicals International (Sigma). L-Aspartate was purchased from Sigma. IVM and MOX were gifts from Fort Dodge Animal Health. All other chemicals and reagents were of the highest purity commercially available.

2.2. Construction of the HcGluCla expression cassette

The complete coding sequence of HcGluCla [17] (GenBank Accession No. AF076682) was amplified by reverse transcriptase-polymerase chain reaction (RT-PCR) from adult *H. contortus* total RNA, using the proofreading DNA polymerase *Pfu* (Stratagene) according to the recommendations of the manufacturer. The sense primer used was 5′-TGT*tctaga***GCCACC**ATGTTCGCCTTGATTCTG-C-3′, and the antisense primer was 5′-CGAgcggccgcTCA *CTTGTCATCGTCGTCCTTGTAGTCC*TCCAACTGTGC-CTGGACT-3′. Restriction sites (lower case italics) were added to the 5′ end of each primer to facilitate subcloning into an expression vector (*Xba*I for the sense primer and *Not*I for the antisense primer). The sense primer also contained a Kozak motif (bold) before the start ATG (underlined) for optimal translation in mammalian cells [27]. For the antisense primer, we also introduced, inframe, 24 nucleotides that encode a C-terminal *FLAG* octapeptide (uppercase italics), DYKDDDDK [28], at the 3′ end before the stop codon (double underline) to allow detection of the expressed receptor, using Western blot analysis. The resulting PCR product was gel-purified, digested with *Xba*I and *Not*I, and ligated to the eukaryotic expression vector pCI-neo (Promega), which was linearized by the same two restriction enzymes. The final constructs were sequenced to confirm correct ligation and orientation.

2.3. Cell culture and transfection

COS-7 cells were maintained at 37° with 5% CO_2 in a humidified incubator. The growth medium was Dulbecco's Modified Eagle's Medium supplemented with 0.02 M HEPES buffer (Biomedia Canada), 10% fetal bovine serum, and 20 μg of gentamicin (Gibco BRL) per 500 mL bottle. For transfection experiments, the HcGluCla–pCI-neo construct was transiently transfected into COS-7 cells using Lipofectamine (Gibco BRL), according to the recommendations of the manufacturer. Briefly, 2.5 μg of construct was mixed with 20 μL of Lipofectamine and added to 10 cm dishes that had been seeded with approximately 10^6 cells 12–15 hr earlier. The medium was changed at 5 and 24 hr post-transfection, and the cells were harvested 40–48 hr later.

2.4. Membrane preparation

The preparation of crude membrane fractions was based on the protocol outlined in [29]. Briefly, cells were washed twice with ice-cold PBS and then incubated in a hypotonic solution (15 mM Tris–HCl, pH 7.4, 1.25 mM $MgCl_2$, 1 mM EDTA) for 10 min at 4°. After swelling, the cells were scraped from the plates, centrifuged at 500 *g* for 5 min at 4°, and resuspended in 5 mL of ice-cold HEPES buffer (pH 7.4) (Fisher Scientific) containing a 1 mM concentration of freshly added phenylmethylsulfonyl fluoride (PMSF) (Sigma). The resuspended cells were lysed on ice by sonication (7 pulses of 15 s on/off), and the lysates were centrifuged at 200 *g* for 5 min at 4°. The supernatant was centrifuged at 28,000 *g* for 20 min at 4°, and the resulting pellet was washed once by resuspension in

ice-cold HEPES and re-centrifuged at 28,000 *g* for 20 min at 4°. The pellet was then resuspended in 50 mM HEPES buffer (pH 7.4), used immediately for protein determination (*via* a Lowry protein determination kit from Sigma) with BSA as a standard, and subsequently stored at −80° at a concentration of 5 μg/μL.

2.5. Western blotting

Approximately 2 μg of membrane protein was subjected to SDS-PAGE electrophoresis on a 10% Tris glycine gel (Novex, Helixx Technologies) and subsequently transferred to a PVDF membrane (Novex, Helixx Technologies). Membranes were blocked with blocking buffer (1 × TBS, 0.1% Tween-20, 5% non-fat milk) overnight at 4° and then incubated with an ANTI-*FLAG* M2 monoclonal antibody (7 μg/mL) (Sigma) for 4 hr at room temperature. The monoclonal antibody reacts specifically with the *FLAG* epitope [28] fused to the C-terminus of HcGluCla. The membrane was washed in 1 × TBS + 0.1% Tween and then incubated with a horseradish peroxidase-conjugated anti-mouse IgG secondary antibody (1:4000 dilution) (Amersham Pharmacia Biotech) for 1 hr at room temperature. Positive bands were detected on X-ray film using Lumilight (Roche Diagnostics).

2.6. [^{3}H]-IVM and [^{3}H]-MOX binding assays

Conditions for the [^{3}H]-MOX and [^{3}H]-IVM binding assays were based on previously established protocols [30,31]. COS-7 membranes (5 μg per reaction) were incubated with a range of [^{3}H]-IVM or [^{3}H]-MOX concentrations in 1 mL of 50 mM HEPES buffer (pH 7.4) containing 0.02% Triton X-100. Reactions were terminated by passage through Whatman GF-B glass fiber filters previously soaked in 50 mM HEPES buffer containing 0.1% polyethyleneimine. Filters were washed three times with 5 mL of ice-cold H_2O containing 0.1% Triton X-100. Non-specific binding was measured in the presence of a 1000-fold molar excess of unlabelled IVM or MOX. Specific binding was measured as a difference between total and non-specific binding. Sample radioactivity was assessed using a Wallac 1414 liquid scintillation counter.

2.7. Data analysis

All binding data were analyzed using a non-linear regression analysis with the Prism 3.0 software package (Graph Pad) according to the methods outlined in the manual. Data from saturation experiments were analyzed using the equation $Y = (B_{max}X)/K_d + X$. K_i values were determined using the Cheng and Prusoff [32] equation $K_i = IC_{50}/(1 + [\text{ligand}]/K_d)$. Comparisons of means were performed using Student's *t*-test, and a P value <0.05 was considered significant.

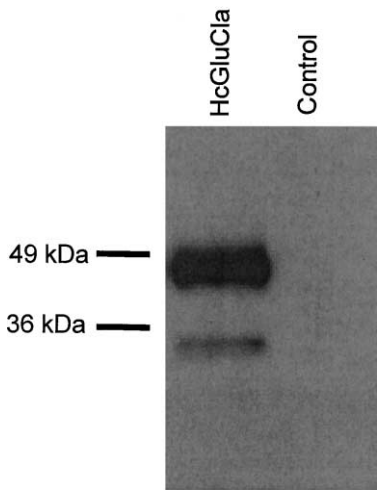

Fig. 1. Western blot analysis of membranes from COS-7 cells transfected with either the pCI-neo vector containing the HcGluCla-*FLAG* cDNA (HcGluCla) or the pCI-neo vector alone (control). The PVDF membrane was treated with the ANTI-*FLAG* M2 monoclonal antibody that targets the *FLAG* epitope fused to HcGluCla.

3. Results

3.1. Transfection of COS-7 cells with HcGluCla

To determine whether the HcGluCla-*FLAG* cDNA could be expressed in COS-7 cells, constructs were transiently transfected into COS-7 cells and analyzed by a preliminary Western blot using an antibody specific for the *FLAG* epitope. The results showed an intense band of approximately 49 kDa, which was expected of a 435 amino acid HcGluCla fragment. A small faint, likely truncated, fragment was also observed at 36 kDa. No band was observed from COS-7 cells transfected with the pCI-neo vector alone (control lane) (Fig. 1).

3.2. Binding assay with [^{3}H]-MOX and [^{3}H]-IVM

In a preliminary experiment, COS-7 cells were transfected with either the pCI-neo vector containing the HcGluCla cDNA or the pCI-neo vector alone. Membranes were then assayed for [^{3}H]-MOX binding. The membranes from cells transfected with the HcGluCla showed strong binding activity, while no activity was observed in cells transfected with the vector alone (control) (Fig. 2). To determine the affinity of [^{3}H]-MOX to HcGluCla, a saturation experiment using various concentrations of [^{3}H]-MOX was conducted. Results showed the existence of a high-affinity [^{3}H]-MOX binding site with a K_d of 0.18 ± 0.016 nM and a B_{max} of 5.5 ± 0.24 pmol/mg protein (Fig. 3A). Scatchard analysis generated a linear plot consistent with a one-site model for the [^{3}H]-MOX binding. This high-affinity macrocyclic lactone binding site also bound [^{3}H]-IVM with a K_d of 0.11 ± 0.021 nM and a B_{max} of 4.9 ± 0.31 pmol/mg protein (Fig. 3A). In displacement

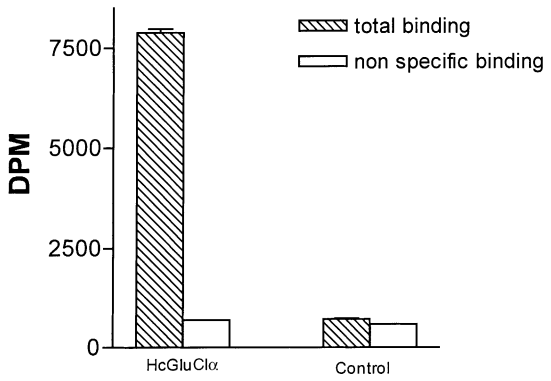

Fig. 2. A preliminary binding experiment showing strong [^{3}H]-MOX binding (total binding vs. non-specific binding) to membranes from cells transfected with pCI-neo vector containing the HcGluCla cDNA compared with those transfected with the vector alone (control). The concentration of [^{3}H]-MOX used was 0.5 nM. Data are expressed as the means ± SEM of three independent experiments, each performed in duplicate.

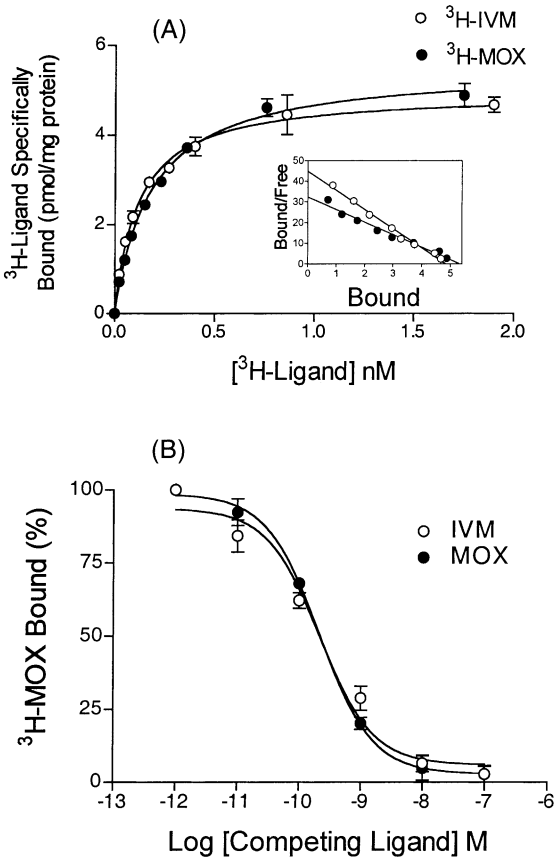

Fig. 3. Specific binding of the macrocyclic lactone anthelmintics [^{3}H]-IVM and [^{3}H]-MOX to HcGluCla. (A) COS-7 membranes were incubated with a range of [^{3}H]-IVM or [^{3}H]-MOX concentrations for 1 hr at room temperature. Non-specific binding was determined using a 1000-fold molar excess of unlabelled IVM or MOX. Inset: scatchard plot for IVM and MOX binding. (B) Displacement analysis of [^{3}H]-MOX using various concentrations of IVM and MOX. Membranes were incubated with 0.45 nM [^{3}H]-MOX for 1 hr at room temperature in the presence of various concentrations of unlabelled MOX and IVM. The representative IC_{50} and K_i values are shown in Table 1. Each point represents the mean ± SEM of three independent experiments, each performed in duplicate.

Table 1
Displacement analysis of [^{3}H]-MOX binding with various concentrations of three competitors

Competitor	IC_{50} (nM)	K_i (nM)
Moxidectin	0.21 ± 0.005	0.061 ± 0.0015
Ivermectin	0.24 ± 0.035	0.068 ± 0.0099
Glutamate	$>10^{-6}$	$>10^{-6}$

Data are expressed as the mean ± SEM of three independent experiments, each performed in duplicate.

experiments, both MOX and IVM completely displaced [^{3}H]-MOX binding (Fig. 3B) and had similar IC_{50} and K_i values (Table 1). Glutamate, however, did not displace either [^{3}H]-IVM (data not shown) or [^{3}H]-MOX (Table 1) even at a concentration of 1 mM.

3.3. Kinetics of [^{3}H]-MOX binding to HcGluCla

Previous work has demonstrated that [^{3}H]-IVM exhibits a time-dependent association to its binding site (likely to be a GluCla subunit) on *C. elegans* membrane preparations and forms an essentially irreversible receptor–ligand complex [30,31]. Therefore, we wanted to determine whether the IVM analog [^{3}H]-MOX exhibits similar kinetic properties when interacting with a recombinant GluCl. To determine the association rate constant of [^{3}H]-MOX binding to HcGluCla, transfected COS-7 membranes were incubated for various intervals with [^{3}H]-MOX in the presence or absence of a 1000-fold molar excess of unlabelled MOX prior to termination. Specific binding increased to reach equilibrium after 15 min and remained stable up to 60 min (Fig. 4A). The mean association rate constant (K^{+1}) from three independent experiments was $2.8 \pm 0.34 \times 10^8$ M^{-1} min^{-1}.

To determine the dissociation rate constant of [^{3}H]-MOX from HcGluCla, transfected COS-7 cells were incubated with [^{3}H]-MOX (0.9 nM) for 60 min to achieve equilibrium binding, after which a 1000-fold molar excess of unlabelled MOX was added; the reactions were terminated at various intervals. Equilibrium-bound [^{3}H]-MOX formed an essentially irreversible complex with HcGluCla. Binding started to plateau after 20 min, and by 60 min after equilibrium 73% of the ligand was still bound (Fig. 4B). Since [^{3}H]-MOX does not completely dissociate from HcGluCla, the dissociation rate constant (K^{-1}) was determined from the initial slope of the line from Fig. 4B, which was 0.065 ± 0.016 min^{-1}. The kinetically derived K_d determined by the equation [$K_d = K^{-1}/K^{+1}$] was 0.23×10^{-9} M, which reflects the K_d derived from saturation analysis (0.18×10^{-9} M) for the [^{3}H]-MOX binding site.

3.4. Interaction between glutamate and [^{3}H]-MOX on HcGluCla

Both functional [6,7,13] and binding studies [26] have shown that IVM influences glutamate activity, possibly through an allosteric interaction from a distinct binding site

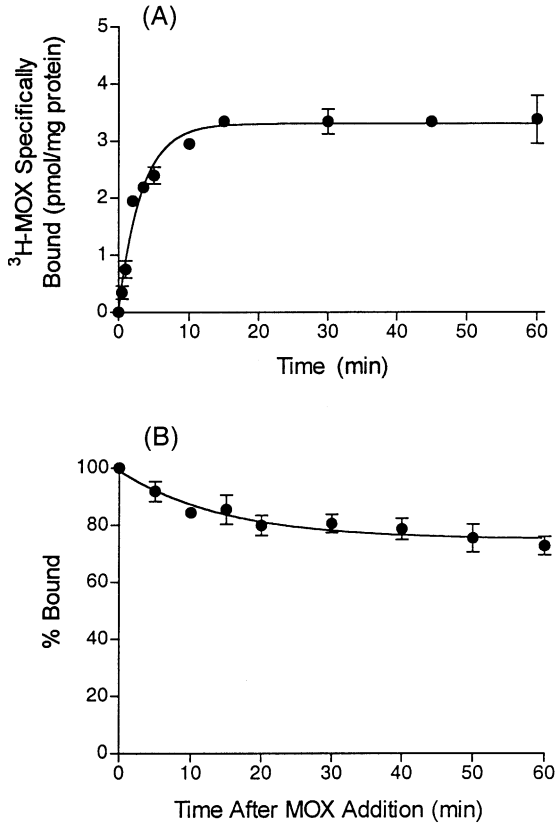

Fig. 4. Kinetics of [^{3}H]-MOX binding to HcGluCla. (A) Association: specific binding of [^{3}H]-MOX (0.9 nM) was measured as a function of time in the presence or absence of a 1000-fold molar excess of unlabelled MOX. (B) Dissociation: [^{3}H]-MOX (0.9 nM) was incubated with membranes for 60 min at room temperature to achieve equilibrium binding, after which a 1000-fold molar excess of unlabelled MOX was added and the reactions were terminated at the indicated times. All points are the means ± SEM of three independent experiments, each performed in duplicate.

on the GluCl. However, it is not known whether glutamate has any influence on either IVM or MOX binding. The possibility that glutamate may affect allosterically [^{3}H]-MOX binding was examined by performing [^{3}H]-MOX saturation experiments in the presence or absence of 10 μM glutamate. The application of glutamate enhanced the affinity of [^{3}H]-MOX significantly by decreasing the K_d approximately 50% from 0.206 ± 0.01 nM (untreated) to 0.136 ± 0.016 nM (glutamate-treated) ($P = 0.02$) (Fig. 5A) but had no significant effect on the B_{max} [14.4 ± 1.3 (untreated), 19 ± 4.1 pmol/mg protein (glutamate-treated)] ($P = 0.34$). Glutamate also had a concentration-dependent effect on [^{3}H]-MOX binding (Fig. 5B). In concentration–response experiments, we used 0.09 nM [^{3}H]-MOX to achieve both sufficient dpm and a large measurable difference in binding between glutamate-treated and untreated experiments. The EC_{50} value for glutamate potentiation of [^{3}H]-MOX binding was 0.28 ± 0.035 μM.

Previous studies have shown that glutamate can directly open the GluCl channel from *C. elegans* [7] or *D. melanogaster* [13]. However, this same channel is not opened

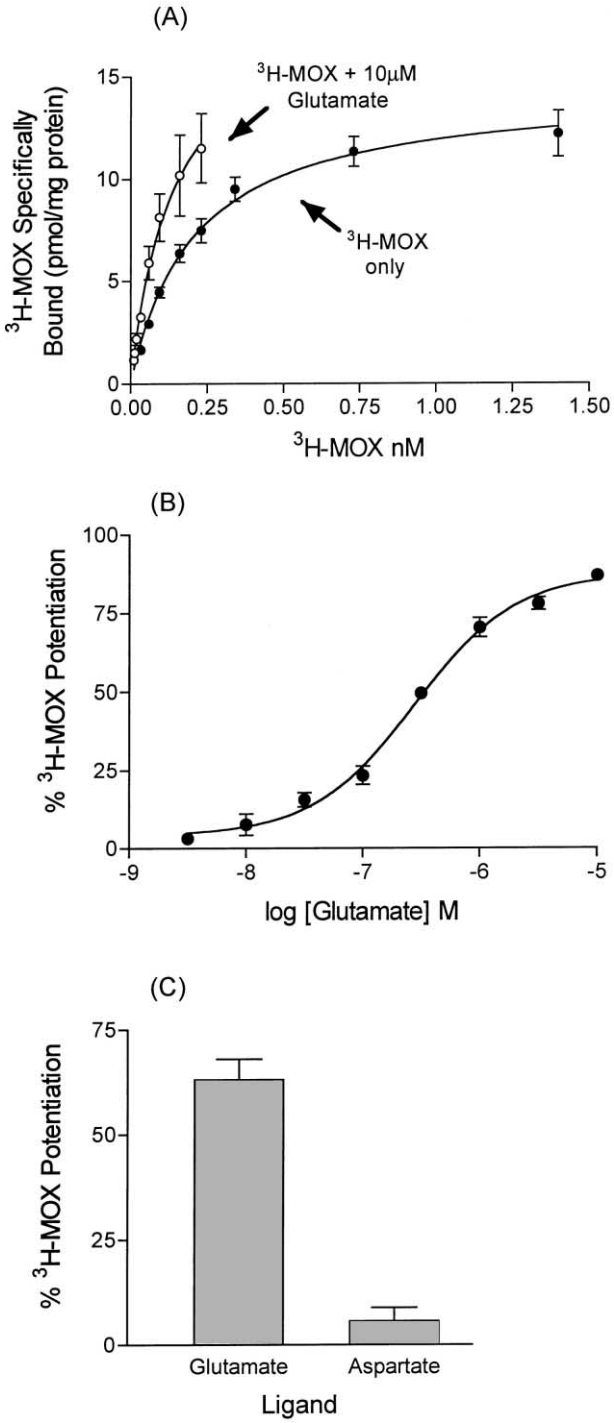

Fig. 5. Glutamate potentiation of [^{3}H]-MOX binding to HcGluCla. (A) [^{3}H]-MOX saturation experiments were performed in the presence (○) or absence (●) of 10 μM glutamate. (B) Concentration–response curve. Data are expressed as percent potentiation above basal ((specific binding + glutamate/basal specific binding − 1) × 100) and were fitted to a single-site sigmoidal concentration–response curve. (C) Effect of aspartate on [^{3}H]-MOX binding. Each ligand (320 nM) was applied with 0.09 nM [^{3}H]-MOX. Data are expressed as percent potentiation above basal. All values are the means ± SEM of three independent experiments, each performed in duplicate.

by aspartate, a structurally similar ligand. Therefore, it is possible that aspartate has no effect on [^{3}H]-MOX binding. To examine this, we compared the effects of glutamate and

aspartate (concentration of 320 nM) on [^{3}H]-MOX binding. While we found that glutamate potentiated [^{3}H]-MOX binding, aspartate had little or no effect (Fig. 5C).

3.5. Interaction between glutamate and [^{3}H]-IVM on HcGluCla

For comparison purposes, we wanted to determine whether glutamate has an effect on [^{3}H]-IVM binding similar to that on [^{3}H]-MOX binding. We found that the application of glutamate had a much stronger effect on [^{3}H]-IVM than on [^{3}H]-MOX binding. Glutamate at 10 μM significantly decreased the K_d for [^{3}H]-IVM binding by more than 7-fold from 0.116 ± 0.009 (untreated) to 0.016 ± 0.0003 nM (glutamate-treated) ($P = 0.0005$) but had no effect on the B_{max} (2.35 ± 0.18 (untreated), 2.38 ± 0.03 pmol/mg protein (glutamate-treated)) ($P = 0.87$) (Fig. 6A). Surprisingly, lower potentation was observed with the application of 1 mM glutamate, which significantly decreased the K_d for [^{3}H]-IVM approximately 3-fold, from 0.1 ± 0.01 (untreated) to 0.03 ± 0.004 nM (glutamate-treated) ($P = 0.0015$) but again had no effect on the B_{max} (2.97 ± 0.06 (untreated), 2.9 ± 0.12 pmol/mg protein (glutamate-treated)) ($P = 0.49$) (Fig. 6B). Maximum potentiation of [^{3}H]-IVM binding (93–100%) using 0.09 nM [^{3}H]-IVM was observed with the application of between 1 and 32 μM glutamate but dropped to 73% when 1 mM glutamate was applied (Fig. 6C). The EC_{50} value for glutamate potentiation of [^{3}H]-IVM binding was 0.094 ± 0.01 μM. In addition, similar to the results with [^{3}H]-MOX, aspartate had little or no effect on [^{3}H]-IVM binding (data not shown).

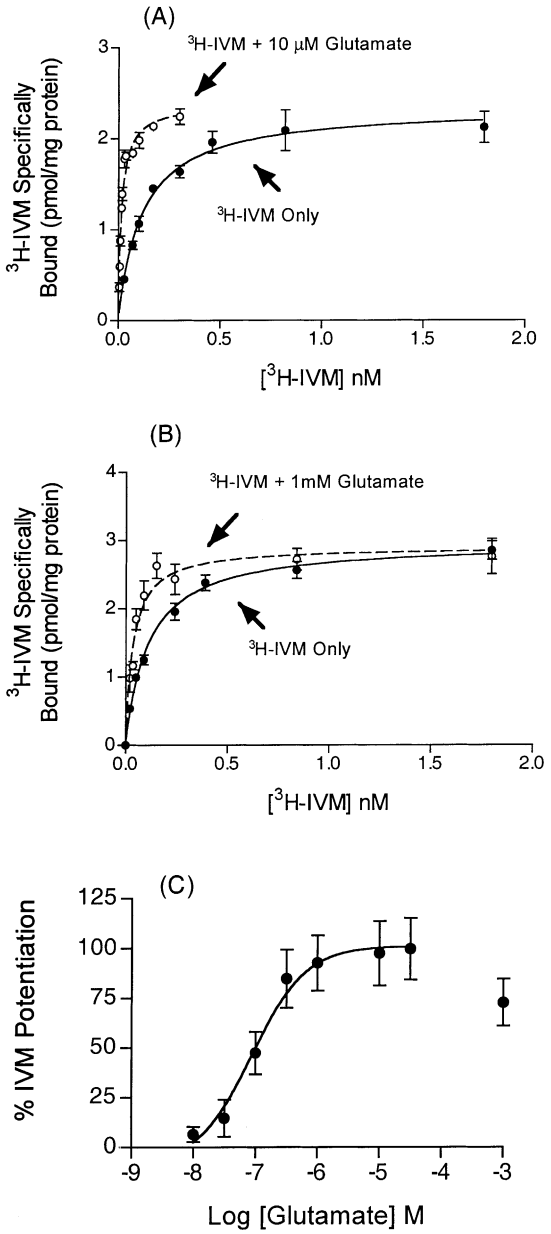

Fig. 6. Glutamate potentiation of [^{3}H]-IVM binding to HcGluCla. (A) [^{3}H]-IVM saturation experiments were performed in the presence (○) or absence (●) of 10 μM glutamate. (B) [^{3}H]-IVM saturation curves were performed in the presence (○) or absence (●) of 1 mM glutamate. (C) Concentration–response curve. Data are expressed as percent potentiation above basal ((specific binding + glutamate/basal specific binding − 1) × 100) and were fitted to a single-site sigmoidal concentration–response curve. All values are the means ± SEM of three or four independent experiments, each performed in duplicate.

4. Discussion

GluCls are members of the ligand-gated ion channel superfamily that includes the $GABA_A$ receptor [2]. Each subunit consists of a large N-terminal extracellular domain and four hydrophobic membrane spanning regions [3]. The glutamate binding site lies most likely in the large N-terminal domain [33], but its general location remains to be determined. Likewise, the location of the IVM binding site is unknown. IVM is known to interact with and modulate a number of ligand-gated ion channels [7,34–36] and therefore may bind to some highly conserved regions within the ligand-gated ion channel family. Localizing the macrocyclic lactone binding site may provide further information on the properties of these molecules and the channels they target.

We have shown that HcGluCla exhibits a high-affinity binding site for the avermectin [^{3}H]-IVM and the milbemycin [^{3}H]-MOX, with binding affinities similar to those observed for IVM in *C. elegans* [30,31] and *H. contortus* [37] membrane preparations and most recently in COS-7 cells expressing HcGluCla [38]. Both anthelmintics fully displace [^{3}H]-MOX binding, providing strong evidence that IVM and MOX bind to a common site on the channel that is distinct from the glutamate binding site. In addition, kinetic analysis of the [^{3}H]-MOX binding site on HcGluCla revealed properties similar to those of the previously reported [^{3}H]-IVM binding site from *C. elegans* membrane preparations [30,31]. As in previous studies with IVM, we observed that [^{3}H]-MOX did not dissociate significantly from its binding site on the GluCl. This is consistent with the fact that these molecules cause an essentially irreversible

chloride current when applied to GluCls, *in vitro* [5–7] and *in vivo* [14]. Both the avermectins and the milbemycins share a 16-membered macrocyclic unit but differ in the fact that the avermectins possess a disaccharide substituent at C-13 [22]. However, given the similarities in these binding characteristics between IVM and MOX, it is likely that these drugs share strong similarities in their modes of action. However, it is interesting to note that while it has been shown that MOX is more potent than IVM *in vivo* [39], our results suggest that the two compounds have similar affinities for the GluCl. Possibly the difference in the pharmacokinetic behavior of IVM and MOX [40] has an influence on their potency.

An interaction between IVM and glutamate has been demonstrated previously using *Xenopus*-expressed *C. elegans* GluCls [6,7]. These authors showed that low concentrations of IVM can potentiate the glutamate response. Since we were unable to obtain specific binding of [^{3}H]-L-glutamate, we were unable to examine the effect of IVM on L-glutamate binding. However, we did observe that low to moderate concentrations of glutamate can potentiate IVM and MOX binding significantly. In a recent study Paiement *et al.* [41] reported that glutamate reduces the inhibition of pharyngeal pumping by IVM and MOX in *H. contortus* at a site that is likely to be a GluCl. These inhibitory effects of glutamate were also different between unselected and IVM-resistant worms and between IVM and MOX in unselected worms. Interestingly, we have also shown differences between IVM and MOX in their interaction with glutamate on a recombinant GluCl, suggesting that there are differences in the activity of these anthelmintics. The mechanism of IVM/MOX potentiation by glutamate is unknown, and whether this potentiation has any effect on the efficacy of IVM or MOX *in vivo* is also unknown.

The potentiation of IVM and MOX is likely due to changes in the receptor that occur through the binding of glutamate to a distinct binding site. We feel that given the dramatic increase in IVM affinity in the presence of glutamate, there must be a major shift in the conformation of the channel when glutamate binds. It is possible that when glutamate binds to HcGluCla, it induces an open-channel conformational state that enhances IVM/MOX binding. Since aspartate does not open the GluCl [7], it may explain why aspartate showed no effect on IVM and MOX binding. Finally, since IVM itself can directly open the GluCl through binding to the α-subunit, what effect, if any, does an IVM-induced conformational change have on the IVM binding site? Binding studies have shown evidence that IVM binds to its receptor in a two-state manner [30]: the first state a low-affinity state that can readily dissociate from the binding site, and the second a high-affinity state that exhibits essentially irreversible binding. However, how these states of binding relate to IVM channel opening is still unknown.

We have shown, for the first time, evidence for the enhancement of anthelmintic binding by ligands acting allosterically at the same receptor. This study further contributes to the understanding of the mode of action of IVM and MOX in parasitic nematodes. With further characterization of these IVM receptors, we may better understand the mechanism of IVM resistance.

Acknowledgments

The technical assistance of C. Trudeau and the constructive suggestions of P. Ribero, F. Hamdan, and C. Allison are greatly appreciated. The critical review of this manuscript by C. Allison and two anonymous reviewers was helpful and appreciated. This work was supported by grants from NSERC, Fonds FCAR, Fort Dodge Animal Health, and the Onchocerciasis Control Program in West Africa Macrofil Chemotherapy project. S. Forrester is the recipient of a post-graduate scholarship from the Natural Sciences and Engineering Research Council of Canada (NSERC) and a McGill Major Fellowship.

References

[1] Arena JP. Expression of *Caenorhabditis elegans* mRNA in *Xenopus* oocytes: a model system to study the mechanism of action of avermectins. Parasitol Today 1994;10:35–7.
[2] Cleland TA. Inhibitory glutamate receptor channels. Mol Neurobiol 1996;13:97–136.
[3] Cully DF, Wilkinson H, Vassilatis DK, Etter A, Arena JP. Molecular biology and electrophysiology of glutamate-gated chloride channels of invertebrates. Parasitology 1996;113(Suppl):S191–200.
[4] Wolstenholme AJ. Glutamate-gated chloride channels in *Caenorhabditis elegans* and parasitic nematodes. Biochem Soc Trans 1997; 25:830–4.
[5] Arena JP, Liu KK, Paress PS, Cully DF. Ivermectin-sensitive chloride currents induced by *Caenorhabditis elegans* RNA in *Xenopus* oocytes. Mol Pharmacol 1991;40:368–74.
[6] Arena JP, Liu KK, Paress PS, Schaeffer JM, Cully DF. Expression of a glutamate-activated chloride current in *Xenopus* oocytes injected with *Caenorhabditis elegans* RNA: evidence for the modulation by avermectin. Mol Brain Res 1992;15:339–48.
[7] Cully DF, Vassilatis DK, Liu KK, Paress PS, van der Ploeg LHT, Schaeffer JM, Arena JP. Cloning of an avermectin-sensitive glutamate-gated chloride channel from *Caenorhabditis elegans*. Nature 1994;371:707–11.
[8] Arena JP, Liu KK, Paress PS, Frazier EG, Cully DF, Mrozik H, Schaeffer JM. The mechanism of action of avermectins in *Caenorhabditis elegans*: correlation between activation of glutamate sensitive chloride current, membrane binding, and biological activity. J Parasitol 1995;81:286–94.
[9] Vassilatis DK, Arena JP, Plasterk RHA, Wilkinson HA, Schaeffer JM, Cully DF, van der Ploeg LHT. Genetic and biochemical evidence for a novel avermectin-sensitive chloride channel in *Caenorhabditis elegans*: isolation and characterization. J Biol Chem 1997;272: 33167–74.
[10] Dent JA, Davis MW, Avery L. *avr*-15 encodes a chloride channel subunit that mediates inhibitory glutamatergic neurotransmission and ivermectin sensitivity in *Caenorhabditis elegans*. EMBO J 1997;16: 5867–79.
[11] Laughton DL, Lunt GG, Wolstenholme AJ. Alternative splicing of a *Caenorhabditis elegans* gene produces two novel inhibitory amino

acid receptor subunits with identical ligand binding domains but different ion channels. Gene 1997;201:119–25.

[12] Dent JA, Smith MM, Vassilatis DK, Avery L. The genetics of ivermectin resistance in *Caenorhabditis elegans*. Proc Natl Acad Sci USA 2000;97:2674–9.

[13] Cully DF, Paress PS, Liu KK, Schaeffer JM, Arena JP. Identification of a *Drosophila melanogaster* glutamate-gated chloride channel sensitive to the antiparasitic agent, ivermectin. J Biol Chem 1996; 271:20187–91.

[14] Martin RJ. An electrophysiological preparation of *Ascaris suum* pharyngeal muscle reveals a glutamate-gated chloride channel sensitive to the avermectin analogue, milbemycin D. Parasitology 1996;112:247–52.

[15] Blackhall WJ, Pouliot JF, Prichard RK, Beech RN. *Haemonchus contortus*: selection at a glutamate-gated chloride channel gene in ivermectin- and moxidectin-selected strains. Exp Parasitol 1998; 90:42–8.

[16] Delany NS, Laughton DL, Wolstenholme AJ. Cloning and localization of an ivermectin-receptor related subunit from *Haemonchus contortus*. Mol Biochem Parasitol 1998;97:177–87.

[17] Forrester SG, Hamdan FF, Prichard RK, Beech RN. Cloning, sequencing, and developmental expression levels of a novel glutamate-gated chloride channel homologue in the parasitic nematode, *Haemonchus contortus*. Biochem Biophys Res Commun 1999;254:529–34.

[18] Jagannathan S, Laughton DL, Critten CL, Skinner TM, Horoszok L, Wolstenholme AJ. Ligand-gated chloride channel subunits encoded by the *Haemonchus contortus* and *Ascaris suum* orthologues of the *Caenorhabditis elegans gbr*-2 (*avr*-14) gene. Mol Biochem Parasitol 1999;103:129–40.

[19] Pribilla I, Takagi T, Langosch D, Bormann J, Betz H. The atypical M2 segment of the β-subunit confers picrotoxinin resistance in inhibitory glycine receptor channels. EMBO J 1992;11:4305–11.

[20] Ffrench-Constant RH, Rocheleau TA, Steichen JC, Chalmers AE. A point mutation in a *Drosophila* GABA receptor confers insecticide resistance. Nature 1993;363:449–51.

[21] Etter A, Cully DF, Liu KK, Reiss B, Vassilatis DK, Schaeffer JM, Arena JP. Picrotoxin blockade of invertebrate glutamate-gated chloride channels: subunit dependence and evidence for binding within the pore. J Neurochem 1999;72:318–26.

[22] Shoop WL, Mrozik H, Fisher MH. Structure and activity of avermectins and milbemycins in animal health. Vet Parasitol 1995;59: 139–56.

[23] Craig TM, Hatfield TA, Pankavich JA, Wang GT. Efficacy of moxidectin against an ivermectin-resistant strain of *Haemonchus contortus* in sheep. Vet Parasitol 1992;41:329–33.

[24] Coles GC, Giordano-Fenton DJ, Tritschler II JP. Efficacy of moxidectin against nematodes in naturally infected sheep. Vet Rec 1994; 135:38–9.

[25] Conder GA, Thompson DP, Johnson SS. Demonstration of co-resistance of *Haemonchus contortus* to ivermectin and moxidectin. Vet Rec 1993;132:651–2.

[26] Paiement J-P, Prichard RK, Ribeiro P. *Haemonchus contortus*: characterization of a glutamate binding site in unselected and ivermectin-selected larvae and adults. Exp Parasitol 1999;92:32–9.

[27] Kozak M. Point mutations define a sequence flanking the AUG initiator codon that modulates translation by eukaryotic ribosomes. Cell 1986;44:283–92.

[28] Hopp TP, Prickett KS, Price VL, Libby RT, March CJ, Cerretti DP, Udal DL, Conlon PJ. A short polypeptide marker sequence useful for recombinant protein identification and purification. Biotechnology 1988;6:1204–10.

[29] Hamdan FF, Ungrin MD, Abramovitz M, Ribeiro P. Characterization of a novel serotonin receptor from *Caenorhabditis elegans*: cloning and expression of two splice variants. J Neurochem 1999;72:1372–83.

[30] Schaeffer JM, Haines HW. Avermectin binding in *Caenorhabditis elegans*: a two-state model for the avermectin binding site. Biochem Pharmacol 1989;38:2329–38.

[31] Cully DF, Paress PS. Solublization and characterization of a high-affinity ivermectin binding site from *Caenorhabditis elegans*. Mol Pharmacol 1991;40:326–32.

[32] Cheng Y-C, Prusoff WH. Relationship between the inhibition constant (K_i) and the concentration of inhibitor which causes 50% inhibition (I_{50}) of an enzymatic reaction. Biochem Pharmacol 1973;22:3099–108.

[33] Etter A, Cully DF, Schaeffer JM, Liu KK, Arena JP. An amino acid substitution in the pore region of a glutamate-gated chloride channel enables the coupling of ligand binding to channel gating. J Biol Chem 1996;271:16035–9.

[34] Graham D, Pfeiffer F, Betz H. Avermectin B_{1a} inhibits the binding of strychnine to the glycine receptor of rat spinal cord. Neurosci Lett 1982;29:173–6.

[35] Sigel E, Baur R. Effect of avermectin B_{1a} on chick neuronal γ-aminobutyrate receptor channels expressed in *Xenopus* oocytes. Mol Pharmacol 1987;32:749–52.

[36] Krause RM, Buisson B, Bertrand S, Corringer P-J, Galzi J-L, Changeux J-P, Bertrand D. Ivermectin: a positive allosteric effector of the α-7 neuronal nicotinic acetylcholine receptor. Mol Pharmacol 1998;53:283–94.

[37] Rohrer SP, Birzin ET, Eary CH, Schaeffer JM, Shoop WL. Ivermectin binding sites in sensitive and resistant *Haemonchus contortus*. J Parasitol 1994;80:493–7.

[38] Cheeseman CL, Delany NS, Woods DJ, Wolstenholme AJ. High-affinity ivermectin binding to recombinant subunits of the *Haemonchus contortus* glutamate-gated chloride channel. Mol Biochem Parasitol 2001;114:161–8.

[39] Molento MB, Wang GT, Prichard RK. Decreased ivermectin and moxidectin sensitivity in *Haemonchus contortus* selected with moxidectin over 14 generations. Vet Parasitol 1999;86:77–81.

[40] Lanusse C, Lifschitz A, Virkel G, Alvarez L, Sanchez S, Sutra JF, Galtier P, Alvinere M. Comparative plasma disposition kinetics of ivermectin, moxidectin and doramectin in cattle. J Vet Pharmacol Ther 1997;20:91–9.

[41] Paiement J-P, Leger C, Ribeiro P, Prichard RK. *Haemonchus contortus*: effects of glutamate, ivermectin, and moxidectin on inulin uptake activity in unselected and ivermectin-selected adults. Exp Parasitol 1999;92:193–8.